

Absolute keV photon yields from ultrashort laser-field-induced hot nanoplasmas

S. Dobosz, M. Lezius, M. Schmidt, P. Meynadier, M. Perdrix, and D. Normand
CEA-DSM/DRECAM/SPAM, Centre d'Etudes Nucléaire de Saclay, Bâtiment. 524, 91191 Gif-sur-Yvette Cedex, France

J.-P. Rozet and D. Vernhet
GPS-PIIM, Université de Paris VII et Paris VI, 2 place Jussieu, 75251 Paris Cedex 05, France
(Received 18 June 1997)

We study the x-ray L -shell production from large krypton clusters submitted to ultrashort and intense laser pulses. The x-ray photon emission pattern appears to be isotropic and the absolute x-ray photon yields per laser pulse are measured as a function of the laser intensity and of the estimated mean cluster size in the supersonic expansion. In particular, up to 4×10^6 x-ray photons per laser shot are detected at intensities approaching 5×10^{17} W cm $^{-2}$. This allows us to determine precisely a maximum conversion efficiency of 1.7×10^{-8} between the incoming IR photon and the generated x-ray photon energies. Finally, the x-ray photon emission is understood as the result of highly stripped ion production with L -shell electron-impact ionization and excitation in laser-heated cluster-sized nanoplasmas. [S1050-2947(97)51010-9]

PACS number(s): 52.50.Jm, 34.80.Kw, 36.40.c, 52.25.Nr

Since the advent of intense pulsed lasers, the strong field interaction with matter has become a field of active research [1]. An important feature is the generation of soft and hard x rays from laser-produced hot and short-lived plasmas. In particular, the irradiation of solid targets with ultrashort laser pulses, allowing the generation of copious x-ray bursts down to the subpicosecond time scale, has been extensively studied [2]. Recently, using rare-gas cluster beams instead of solids, efficient generation of x rays in the keV range [3] and of soft x rays (< 500 eV) [4,5] has been reported. This observation is of considerable interest, since cluster beams represent a promising, since renewable, target that is easy to handle and that could allow future applications of ultrashort x-ray pulses, such as time-resolved x-ray microscopy [6]. So far, keV x rays emitted from clusters have mainly been identified spectroscopically. However, for future applications it is essential to measure conversion efficiencies and emission patterns and to get a precise knowledge of the parameters allowing optimization of the x-ray photon yields. We present here a systematic experimental study of x-ray generation from large krypton clusters when submitted to intense and ultrashort infrared laser pulses. In particular, the L -shell photon emission is characterized using highly efficient semiconductor detectors instead of the commonly used crystal spectrographs in studies of strong laser matter interaction [3]. We have measured the absolute x-ray L -shell photon yield as a function of the laser intensity and of the stagnant pressure of the cluster source. Moreover, the emission pattern of the energetic radiation is determined. The results of our study suggest a mechanism for the x-ray production arising from electron-impact ionization (EII) and excitation (EIE) of atoms in the laser-heated cluster-sized nanoplasmas [4,5,7-9] and resulting in highly stripped ions with L -shell vacancies.

The experimental setup, including the apparatus used for cluster generation, has been described in detail in a previous publication [7]. Briefly, clusters are generated within a pulsed adiabatic expansion. The intense laser field is generated with a Ti:sapphire laser system delivering 130 fs pulses at 790 nm with a repetition rate of 20 Hz. The beam diameter

is approximately 45 mm and the maximum pulse energy available in the interaction zone is 83.5 mJ. The laser light is focused with an $f=170$ mm off-axis parabolic mirror leading to a maximum peak intensity $I_{\text{peak}} \approx 5 \times 10^{17}$ W cm $^{-2}$. The I_{peak} values are determined from the saturation intensities in the optical field ionization (OFI) of a low-density atomic neon target using the barrier suppression ionization model [10,11]. The precision of this method is estimated to be $\pm 20\%$.

An essential basis for the present investigation of x-ray yields is the characterization of the cluster beam target. Estimation of the mean cluster size \bar{N}_{Kr} can be obtained from the results of a detailed, systematic study of Hagena and Obert [12]. These authors have measured the mean cluster sizes for different expansion conditions, i.e., at different stagnant pressures P_0 and initial gas temperatures T_0 , using a pulsed supersonic expansion through a $\phi_n = 150$ μm conical nozzle with a length of 25 mm. We use an identical cluster source in our experiment with typical valve opening times of 400 μs . For this reason, the data supplied by Ref. [12] as well as by Farges *et al.* [13] enable us to estimate the mean cluster size \bar{N}_{Kr} from the empirical value Γ^* in the present experiment:

$$\Gamma^* = k \frac{P_0 [\text{mbar}]}{(T_0 [\text{K}])^{2.29}} \left(\frac{\phi_n [\mu\text{m}]}{\tan \alpha} \right)^{0.85}, \quad (1)$$

$$\bar{N}_{\text{Kr}} \approx A_0 (\Gamma^*)^{1.95}. \quad (2)$$

The dimensionless constant k , depending on the atomic species, is equal to 2900 for krypton, the half opening angle of the jet α is taken as 5° , and A_0 is determined according to Ref. [13] to 2.5×10^{-4} . With Eqs. (1) and (2) and assuming $T_0 = 298$ K, we determine the average cluster size to $\bar{N}_{\text{Kr}} = 5 \times 10^4$ at $P_0 = 5$ bar and $\bar{N}_{\text{Kr}} = 7 \times 10^5$ at $P_0 = 20$ bar. According to Ref. [14], the atomic beam density ρ_{Kr} within the target region follows a linear dependence on the stagnant pressure:

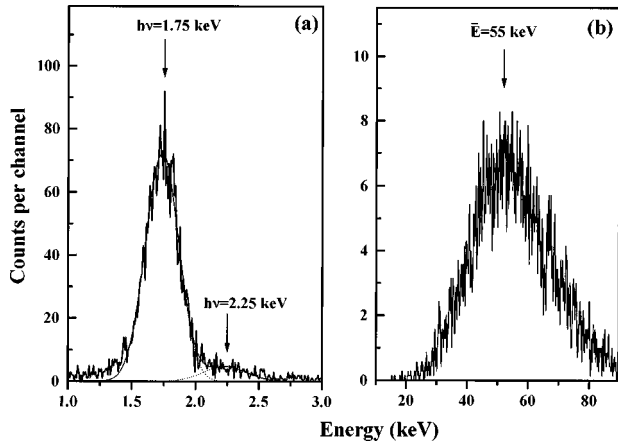


FIG. 1. X-ray spectra obtained after irradiation of large krypton clusters ($\bar{N}_{\text{Kr}}=5 \times 10^5$) with 130-fs infrared pulses at 790 nm using a peak intensity of $4 \times 10^{17} \text{ W cm}^{-2}$. Spectrum (a) is recorded at a reduced count rate by using a diaphragm in front of the detector, whereas (b) is obtained without a diaphragm.

$$\rho_{\text{Kr}} [\text{cm}^{-3}] = A_1 \times (P_0 [\text{bar}]) \quad (3)$$

In our case the constant A_1 evaluates to $A_1 = 1.4 \times 10^{13} \text{ cm}^{-3} \text{ bar}^{-1}$. This value is in good agreement with target density measurements as a function of backing pressure obtained from the total ion currents produced by OFI [15].

The x rays are analyzed using two Si(Li) semiconductor detectors of well-known characteristics [16–18]. These detectors have a 10-mm active diameter and are sealed with thin (25- μm) Be windows. Energetic electrons and ions are absorbed, but x rays ($h\nu > 1 \text{ keV}$) are efficiently detected. Further energy discrimination of low-energy x rays can be achieved, if necessary, by using thin aluminum-coated Mylar foils in front of the detectors. The solid detection angle is optimized by introducing the detector nozzle into the vacuum chamber close to the interaction zone. The distances of the Si(Li) junctions with respect to the laser focus are typically chosen between 110 mm and 260 mm, leading, respectively, to solid angles of detection Ω_{det} between 6.49×10^{-3} and $1.16 \times 10^{-3} \text{ sr}$. The detectors can be positioned to different angles (0° , 100° , and 145°) with respect to the laser beam. These different arrangements allow us to study the emission pattern of the observed radiation, and to ensure that any detected photon originates from the interaction region, thus excluding the possibility of parasitic photon emission from the impact of energetic electrons or ions on the chamber surfaces. For single-photon spectra, the counting rates can be reduced to less than 0.05 counts per pulse by using a Cu diaphragm with $\phi_d = 300 \mu\text{m}$. For very low counting rates ($\ll 1 h\nu/\text{pulse}$), the detector signal is proportional to the photon energy. The energy resolution is $\approx 160 \text{ eV}$ [full width at half maximum (FWHM)] at 2 keV. For higher counting rates, several photons can be detected within one laser shot, and pileup occurs. In this case, the detector signal is proportional to both the photon energy and the simultaneously detected number of photons. Finally, the x-ray detectors are energy calibrated using low-intensity standard x-ray sources [19].

Two typical x-ray spectra are shown in Fig. 1. Spectra (a) and (b) are recorded at $I_{\text{peak}} = 4 \times 10^{17} \text{ W cm}^{-2}$, using stag-

nant pressures of $P_0 = 18 \text{ bar}$ and 16 bar , respectively. The corresponding mean cluster size \bar{N}_{Kr} is estimated to $\approx 5 \times 10^5$. Spectrum (a) is recorded at a reduced counting rate, close to 0.03 counts per pulse. Two broad spectroscopic features, situated respectively at $1750 \pm 50 \text{ eV}$ and $2250 \pm 50 \text{ eV}$, are visible and are fitted as Gaussian peaks with FWHM $\approx 300 \text{ eV}$. Gauss-type fitting for such line shapes is justified for low counting rates [17]. The line broadening, compared to the detector resolution, indicates the presence of a complex set of lines from highly charged Kr^{q+} ions. For such ions it is well known that the emission lines are shifted towards higher energies compared to those of singly ionized atoms [20,21]. In that respect, the two features in Fig. 1 at 1750 and 2250 eV can be, respectively, assigned to $3\ell \rightarrow 2\ell'$ and $4\ell \rightarrow 2\ell'$ transitions in multi-ionized krypton. Besides, our spectrum corresponds well to the envelope of high-resolution x-ray data [3], where the numerous lines have been assigned to radiative transitions in Kr^{q+} ($q=24-27$).

Spectrum (b) in Fig. 1 is recorded without Cu diaphragm and thus at a much higher counting rate than (a). In this case, an average number of ≈ 31.5 photons are simultaneously detected during each laser pulse. Actually, this spectrum corresponds to a Poissonian distribution around a mean energy $\bar{E} = 55 \text{ keV}$. Using Poissonian statistics, it is easy to show that the mean detected photon number per laser pulse, denoted by \bar{n}_p , is related to this mean energy by

$$\bar{n}_p = \frac{N_{\text{event}}}{N_{\text{laser}}} \frac{\bar{E}}{h\nu}, \quad (4)$$

where $h\nu$ is the mean energy of the one photon spectrum [Fig. 1(a)], N_{event} is the number of recorded events, and N_{laser} is the number of laser shots during acquisition. Such measurements allow an accurate determination of photon yields over three orders of magnitude without any modification of the experimental setup. In order to determine the emission pattern of the energetic photons, we have measured \bar{n}_p for three different positions of the two detectors [22], as well as for horizontal and vertical laser polarization. Clearly, an isotropic emission pattern is observed within the experimental error of $\pm 5\%$. Based on this result the mean photon number per laser pulse emitted over $\Omega = 4\pi$, further denoted by \bar{N}_p , is given by:

$$\bar{N}_p = \frac{\bar{E}}{h\nu} \frac{N_{\text{event}}}{N_{\text{laser}}} \frac{4\pi}{\epsilon \Omega_{\text{det}} T_{\text{My}}} \quad (5)$$

with the overall detector efficiency $\epsilon \approx 0.4$ and the transmission of the Mylar foil $T_{\text{My}} \approx 0.5$. From Fig. 1(b) and Eq. (5), \bar{N}_p is determined to 1.6×10^6 .

In addition, the observation of an isotropic emission pattern shows that the polarization vector of the x-ray photons has a random orientation, in contrast to the well-defined linear polarization of the incident infrared laser photons. Nevertheless, even for highly oriented systems, angular-momentum couplings in many-electron ions may lead to severe depolarization during the emission process [23,24]. The observation of isotropic x-ray emission is also expected in the nanoplasma model [4,5,7–9]. In this model, the inci-

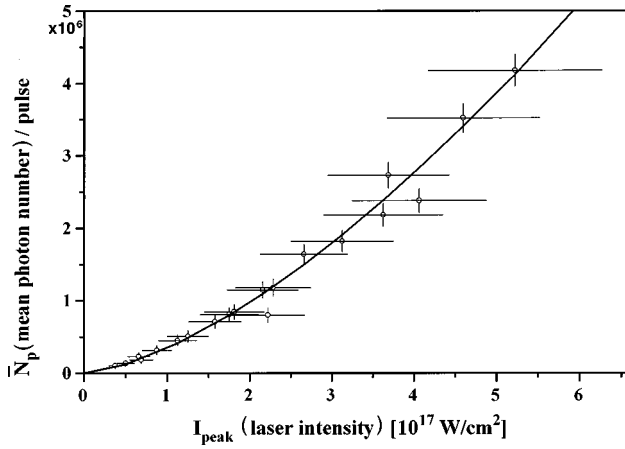


FIG. 2. Measured x-ray photon yields (\bar{N}_p) as a function of the laser peak intensity I_{peak} . The estimated mean cluster size is 7×10^5 at $P_0 = 19.5$ bar. The experimental errors for I_{peak} and \bar{N}_p are indicated.

dent laser beam heats the cluster-sized plasma by inverse bremsstrahlung (IB) and the oscillating, hot electrons induce EII or EIE of the atoms. Obviously, the information on the phase of the incident laser photons is lost in such an excitation mechanism.

We have studied the total photon number per pulse \bar{N}_p as a function of the laser peak intensity I_{peak} . Figure 2 shows the evolution of \bar{N}_p for intensities between 3.7×10^{16} W cm^{-2} and 5.2×10^{17} W cm^{-2} . Analysis of the data indicates that the experimental result is best fitted with

$$\bar{N}_p \propto I_{\text{peak}}^{3/2} \quad (6)$$

A very similar intensity dependence has been observed previously in experiments concerning OFI of rare-gas atoms [25,26]. From these studies it is well known that, as soon as the ion yield of a given charge state enters the saturation regime, the signal increases further with $I_{\text{peak}}^{3/2}$. This behavior is simply due to the increase of the focal volume with increasing I_{peak} . Thus, two important conclusions can be drawn on the basis of Fig. 2. For a given cluster size [$\bar{N}_{\text{Kr}} \approx 6.8 \times 10^5$, using Eqs. (1) and (2)], the process appears to be saturated already at low intensities of 3.7×10^{16} W cm^{-2} , since the increase of \bar{N}_p is solely due to the increase of the focal volume. Then, the onset of the x-ray generation process should occur at even lower intensities ($< 10^{16}$ W cm^{-2}). This interpretation is consistent with results presented in Ref. [27] indicating the production of Kr^{18+} ions from the interaction of krypton clusters with moderately intense laser pulses ($I_{\text{peak}} = 10^{15}$ W cm^{-2}). The detection of such high charge states by means of a mass spectrometer on a microsecond time scale suggests that during the laser pulse much higher charge states are reached in the target and that massive recombination follows during expansion of the plasma. Finally, it is worth mentioning that our findings are at variance with scaling laws, recently proposed in Ref. [3], which suggest threshold intensities exceeding 10^{17} W cm^{-2} for the cluster sizes in our experiment.

The dependence of \bar{N}_p on the stagnant pressure P_0 has also been measured. The resulting data, shown in Fig. 3, can

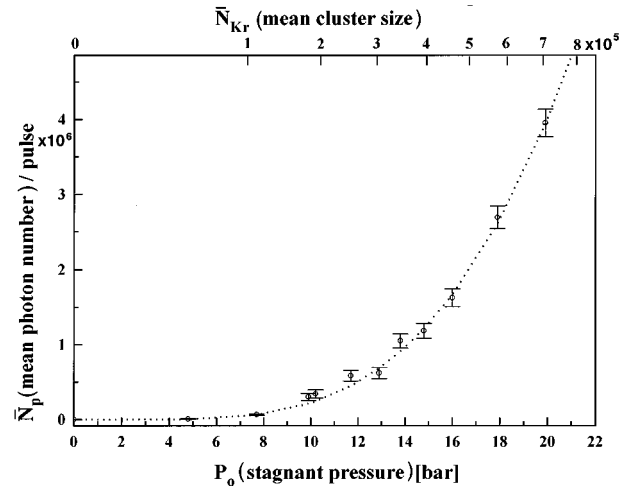


FIG. 3. Measured x-ray photon yields (\bar{N}_p) as a function of the backing pressure P_0 . The respective mean cluster size \bar{N}_{Kr} is indicated on the upper scale. The laser peak intensity is 4×10^{17} W cm^{-2} .

be fitted with

$$\bar{N}_p = (P_0 - P_c)^\kappa, \quad (7)$$

and choosing an exponent κ of 3 ± 0.3 . Using Eqs. (1) and (2), the \bar{N}_{Kr} scale is determined as a function of P_0 and indicated at the top of Fig. 3. Accordingly, the x-ray yield scales as $\bar{N}_{\text{Kr}}^{3/2}$ with the mean cluster size. The P_0^3 pressure dependence can be understood from the following considerations. In first approximation, the number of collisions N_{coll} for electron-ion-impact processes, such as EII and EIE, is proportional to the product of the number of electrons and ions. Thus, N_{coll} in a given cluster increases with P_0^4 [Eqs. (1) and (2)]. As the number of clusters in the focus scales as $1/P_0$ [Eqs. (2) and (3)], the total x-ray L -shell photon yield \bar{N}_p should rise as P_0^3 and thus as $\bar{N}_{\text{Kr}}^{3/2}$.

The onset of the x-ray production in Fig. 3 occurs at a pressure offset of $P_c \approx 3$ bar [Eq. 7]. At this stagnant pressure, the mean cluster size \bar{N}_{Kr} is close to $\approx 10^4$. This value should roughly indicate the minimum cluster size for significant x-ray production in our experimental conditions. If there exists some optimum cluster size, it greatly exceeds 7×10^5 in the case of krypton, since we observe no saturation at the higher stagnant pressures. These observations are again in contrast to earlier conclusions [3], where a rather small Kr_n cluster size $\bar{N}_{\text{Kr}} \approx 200$ is predicted for optimized x-ray L -shell photon generation.

From our precise measurement of the x-ray photon yields, we can extract energy conversion efficiencies (CE's) for the cluster targets in our experiment. For infrared laser pulse energies of 63.5 mJ, we have measured 4×10^6 x-ray photons per laser shot. Thus, the maximum CE in our experiment slightly exceeds 10^{-8} . This value is, however, rather small compared to the CE observed for solid targets, being several orders of magnitude higher [28,29]. The rather low CE observed for cluster beams presumably arises from the low overall target density compared to solids. However, from our results we cannot exclude the fact that, due to the

high local density of clusters together with their small size, laser energy absorption may be higher than for bulk targets with a comparable number of atoms. For efficient x-ray production, we propose that much higher density cluster beams should be employed in the future.

Finally, it is important to emphasize that for cluster irradiation with the second harmonic ($\lambda=395$ nm) instead of the fundamental within the same experimental conditions, i.e., same \bar{N}_{Kr} and I_{peak} , we do not observe a notable change of the x-ray photon yield [30]. This observation suggests that enhanced electronic coupling does not occur for lasers having shorter wavelength down to $\lambda=395$ nm. The recent observations of Kondo *et al.* [31] indicate that substantially higher photon yields are obtained for 300-fs lasers at $\lambda=248$ nm than for 80-fs laser at $\lambda=800$ nm. We suggest that plasma heating is much more efficient for longer pulses and

shorter wavelengths since then IB occurs over many more optical cycles.

In conclusion, our present study demonstrates that irradiation of clusters with short and intense, infrared laser pulses leads to significant production of *L*-shell vacancies in krypton atoms. The resulting energetic x-ray emission occurs isotropically. We do not observe notable laser wavelength effects. Optimization of the x-ray yield can be achieved by increasing the cluster size as well as the density of clusters, and by increasing the target region in the beam.

The authors acknowledge fruitful discussions with Dr. T. Auguste and Dr. P. Monot and the skilled technical assistance of E. Caprin and M. Bougeard. Partial support is provided by the European union (M.L.) (Grant No ERBFMBICT 950421).

-
- [1] *Ultrafast Phenomena VII*, edited by C. B. Harris, E. P. Ippen, G. A. Mourou, and A. H. Zewail (Springer Verlag, Berlin, 1990).
- [2] M. M. Murnane *et al.*, *Science* **251**, 531 (1991); H. M. Milchberg *et al.*, *Phys. Rev. Lett.* **67**, 2654 (1991); P. Audebert *et al.*, *Europhys. Lett.* **19**, 189 (1992); in *X-ray Lasers 1996, Proceedings of the 5th International Conference on X-ray Lasers, Lund*, edited by S. Svanberg and C.-G. Wahlström, IOP Conf. Series No. 151 (Institute of Physics, Bristol, 1996).
- [3] A. McPherson *et al.*, *Phys. Rev. Lett.* **72**, 1810 (1994).
- [4] T. Ditmire *et al.*, *Phys. Rev. Lett.* **75**, 3122 (1995).
- [5] T. Ditmire *et al.*, *Phys. Rev. A* **53**, 3379 (1996).
- [6] *X-ray Microscopy III*, edited by A. G. Michette, G. R. Morrison, and C. J. Buckley, Springer Series in Optical Sciences Vol. 67 (Springer, London, 1990).
- [7] M. Lezius *et al.*, *J. Phys. B* **30**, L251 (1997).
- [8] M. Schmidt and D. Normand, *Phys. World* **10**, 26 (1997).
- [9] C. Wülker *et al.*, *Opt. Commun.* **112**, 21 (1994).
- [10] S. Augst *et al.*, *Phys. Rev. Lett.* **63**, 2212 (1989).
- [11] P. Monot, thèse de doctorat, Université de Paris Sud, Orsay, 1993 (unpublished).
- [12] O. F. Hagena and W. Obert, *J. Chem. Phys.* **56**, 1793 (1972); O. F. Hagena, *Z. Phys. D* **4**, 291 (1987).
- [13] J. Farges *et al.* *J. Chem. Phys.* **84**, 3491 (1986).
- [14] O. F. Hagena, *Surf. Sci.* **106**, 101 (1981).
- [15] M. Lezius *et al.* (unpublished).
- [16] J. L. Campbell and H. H. Jorch, *Nucl. Instrum. Methods* **159**, 163 (1979).
- [17] P. Lechner and L. Strüder, *Nucl. Instrum. Methods Phys. Res. A* **354**, 464 (1995).
- [18] D. Vernhet *et al.*, *J. Phys. B* **21**, 3949 (1988).
- [19] R. B. Firestone, *Table of Isotopes*, edited by V. S. Shirley, C. M. Baglin, S. Y. F. Chu, and J. Zipkin (J. Wiley and Sons, New York, 1996).
- [20] P. H. Mokler, *Phys. Rev. Lett.* **26**, 811 (1971).
- [21] S. N. Soni, *J. Phys. B* **13**, 2859 (1980).
- [22] J.-P. Rozet *et al.*, *Nucl. Instrum. Methods Phys. Res. A* **262**, 84 (1987).
- [23] J. C. Percival and M. J. Seaton, *Philos. Trans. R. Soc. London, Ser. A* **251**, 113 (1958).
- [24] D. Vernhet *et al.*, *Phys. Rev. A* **32**, 1256 (1985).
- [25] A. L'Huillier, thèse de doctorat, Université Pierre et Marie Curie, Paris, 1986 (unpublished).
- [26] T. Auguste *et al.*, *J. Phys. B* **25**, 4181 (1992).
- [27] E. M. Snyder *et al.*, *Phys. Rev. Lett.* **77**, 3347 (1996).
- [28] D. G. Stearns *et al.*, *Phys. Rev. A* **37**, 1684 (1988).
- [29] S. P. Gordon *et al.*, *Opt. Lett.* **19**, 484 (1994).
- [30] S. Dobosz *et al.* (unpublished).
- [31] K. Kondo *et al.*, *J. Phys. B* **30**, 2707 (1997).